LWT - Food Science and Technology 68 (2016) 190–201

Contents lists available at ScienceDirect

LWT - Food Science and Technology

journal homepage: www.elsevier.com/locate/lwt

Impacts of freezing and molecular size on structure, mechanical properties and recrystallization of freeze-thawed polysaccharide gels

Nathdanai Harnkarnsujarit [a, b, *], Kiyoshi Kawai [c], Toru Suzuki [b]

[a] Department of Packaging and Materials Technology, Faculty of Agro-Industry, Kasetsart University, 50 Ngam Wong Wan Rd, Lat Yao, Chatuchak, Bangkok 10900, Thailand
[b] Department of Food Science and Technology, Tokyo University of Marine Science and Technology, 4-5-7, Konan, Minato-ku, Tokyo, Japan
[c] Department of Biofunctional Science and Technology, Graduate School of Biosphere Science, Hiroshima University, 1-4-4 Kagamiyama, Higashi-Hiroshima, Hiroshima, Japan

ARTICLE INFO

Article history:
Received 5 September 2015
Received in revised form
11 December 2015
Accepted 14 December 2015
Available online 17 December 2015

Keywords:
Freezing
Structure
Maltodextrin
Recrystallization
Gel

ABSTRACT

Freezing modifies microstructures and affects physico-chemical changes during thawing of foods. This study investigated impact of freezing temperature (−20 °C, −50 °C and −90 °C) and controlled freezing process, and dextrose equivalent (DE5, DE15 and DE18) of maltodextrin (MD) on microstructure, mechanical and structural changes (shrinkage and recrystallization) of freeze-thawed MD-agar gels. Shrinkage and turbidity of matrices were dependent on freezing conditions and microstructures of solids. X-ray tomography revealed that low cooling rate formed large ice crystals contributed to thicker solid networks. However, a slow cooling to a supercooled region (~0 °C to −1 °C) followed by a quench cooling caused rapid ice nucleation and inhibited ice growths resulting in only few clusters of large ice with a high number of fine ice crystals. Raman spectra indicated amorphous−crystalline transition (recrystallization) of gel components particularly maltodextrin after thawing in low DE systems which increased gel turbidity and subsequently accelerated shrinkage. Lower temperature freezing gave thinner but higher connectivity of solid networks providing higher mechanical strength and delayed recrystallization of maltodextrin which primary increased firmness values. The results indicated that the manipulation of freezing process in achieving small ice crystals effectively reduced structural changes attributing to recrystallization of high DE maltodextrin components in gel systems.

1. Introduction

Freezing is an excellent process to preserve food quality and develop new products i.e. frozen desserts. Ice morphology plays significant role in textural and physical properties of frozen foods. Size and location of ice crystals are keys in the quality of thawed products. Cooling rate is the most common variable controlling ice morphology in frozen and partly frozen systems (Petzold & Aguilera, 2009). Freezing affects microstructures and subsequent changes of food properties such as syneresis and drip loss in freeze-thawed tissues (Kidmose & Martens, 1999; Ngapo, Babare, Reynolds, & Mawson, 1999), texture and firmness of agriculture products (Kidmose & Martens, 1999; Miles, Morris, Orford & Ring; 1985; Sigurgisladottir, Ingvarsdottir, Torrissen, Cardinal, & Hafsteinsson, 2000; Badii & Howell, 2002) and increased toughness of meat (Badii & Howell, 2002) as well as accelerated protein denaturation (Benjakul, Visessanguan, Thongkaew, & Tanaka, 2003; Mackie, 1993; Tironi, Tomás, & Añón, 2010). The structural changes in frozen foods take place during freezing, storage and subsequent thawing. A rapid freezing forms small ice crystals and has been proved to reduce structural changes of frozen foods during storage and thawing. Accordingly, the controlled freezing condition to achieve small ice crystals is essential for frozen food industries. A faster cooling rate can be easily achieved by reduced freezing temperature in conventional freezer. In the present study, a control freezing protocol was used to achieve a rapid freezing after a slow cooling into the supercooled region below equilibrium freezing point.

The destabilization of food gels due to freezing such as drip loss

* Corresponding author. Department of Packaging and Materials Technology, Faculty of Agro-Industry, Kasetsart University, 50 Ngam Wong Wan Rd, Lat Yao, Chatuchak, Bangkok 10900, Thailand.
E-mail address: nathdanai.h@ku.ac.th (N. Harnkarnsujarit).

http://dx.doi.org/10.1016/j.lwt.2015.12.030
0023-6438/

and shrinkage significantly causes adverse effects to frozen products after thawing. Several studies indicated that freezing and thawing modify microstructures and accelerates retrogradation of starch gels (Charoenrein & Preechathammawong, 2010; Kim, Kim, & Shin, 1997; Lee, Baek, Cha, Park, & Lim, 2002; Muadklay & Charoenrein, 2008). The retrogradation of freeze-thawed starch gels led to the release of water adsorbed in the network of starch matrices or so called 'syneresis'. Consequently, the shrinkage of the gels occur as liquid drains from the pores of the matrices (Scherer, 1993). Addition of some food additives such as polysaccharides e.g. gums and maltodextrin has been proved to increase stability of some frozen products (Goff, 1995). Maltodextrin has wide food applications such as carrier for encapsulated components i.e. flavor and bioactive compounds, provide full-fat texture to reduced-fat formulations or fat replacer, modify structures for superior mouthfeel in frozen food and desserts with a lower cost (Chronakis, 1998; Gibbs, Kermasha, Alli, Catherine, & Mulligan, 1999; Setser & Racette, 1992). Previous study showed that various dextrose equivalent (DE) of maltodextrin controlled microstructure formation of freeze-dried matrices which attributed to the manipulation of unfrozen water and ice fraction (Harnkarnsujarit, Charoenrein, & Roos, 2012). Moreover, Rojas, Rosell, and de Barber (2001) showed that maltodextrins of low degree of polymerization (DP) and hence high DE effectively retarded staling of starch gels; however, lack of study revealed the effect of maltodextrin as well as their DE on structure properties of gel matrices after thawing. The structural changes of freeze-thawed systems which majorly contain maltodextrin and freezing effects have also rarely been investigated.

The amorphous starch component is thermodynamically non-equilibrium material and tends to recrystallize which can be measured by using various methods such as differential scanning calorimetry (DSC), X-ray diffraction, spectroscopic and turbidimetric methods (Karim, Norziah, & Seow, 2000). The DSC measures the energy required to disintegrate crystalline fraction relating to the degree of crystallinity which destroys the samples. While some other spectroscopic methods including infrared and Raman spectroscopy are non-destructive and can be used in on-line monitoring of structural changes of food products including retrogradation of amylose and amylopectin in starch components (Bulkin, Kwak, & Dea, 1987; Fechner, Wartewig, Kleinebudde, & Neubert, 2005; Li-Chan, 1996; Schuster, Ehmoser, Gapes, & Lendl, 2000). Raman spectroscopy is based on the distinct vibrational transitions that occur in the ground electronic state of molecules attributes to various stretching and bending deformation modes of individual chemical bonds (Li-Chan, 1996). The sample is radiated with a monochromatic visible or near infrared light from a laser giving the vibrational energy levels in the molecule to a short-lived, high-energy collision state. The activated molecules return to a lower energy state by emission of photon which has a lower frequency than the laser light. The difference between the frequency of the laser and that of the scattered photon is called the Raman shift given in reciprocal centimetres (Thygesen, Løkke, Micklander, & Engelsen, 2003).

The objectives of this study were to determine the effect of freezing on microstructure formations of maltodextrin-agar matrices and subsequent impacts on structural changes upon thawing. Moreover, the structural changes of freeze-thawed maltodextrin with various DE (DE5, DE15 and DE18) were investigated. Agar was formulated to form gel matrices mimicking semi-solid food structures. The findings give benefits to frozen food industry on manipulating freezing process and carbohydrate-based components in achieving highest food stability upon thawing.

2. Materials and methods

2.1. Maltodextrin-agar gels preparation

Maltodextrin (DE5, DE15 and DE18) and agar powders were purchased from Sigma–Aldrich Japan G.K. (Tokyo, Japan) and Wako Pure Chemical Co., Ltd. (Osaka, Japan), respectively. Solid mixtures (15 g/100 g) of maltodextirn-agar (9:1) were dispersed in distilled water (Water distillation apparatus RFD 240RA, Advantec®, Toyo Seisakusho Kaisha Ltd., Osaka, Japan). The maltodextrin-agar suspensions were stirred at 25 °C for 20 min using magnetic stirrer to allow for water adsorption of solids prior to heating to 90 °C and held for 5 min to ensure complete melting of agar. The mixtures were cooled, then poured into containers and left for gelation at 25 °C for 2 h.

2.2. Freezing and thawing

Gels containing maltodextrin were cut into 1-cm cubic and placed on aluminium trays prior to freezing. The freezing conditions composed of conventional chest freezers at −20 °C (dimension of 60 × 80 × 120 cm, SCR-R451G, Sanyo, Japan), −50 °C (dimension of 70 × 80 × 130 cm, Ultra Low, Sanyo, Japan) and −90 °C (dimension of 60 × 50 × 90 cm, MDF-C8v1, Sanyo, Japan) and three controlled freezing protocols using a program freezer (Taiyo Nippon Sanso Corporation, Tokyo, Japan) equipped with liquid nitrogen vessel. A pilot scale program freezer composed of a stainless steel freezing chamber (approximate dimension of 20 × 30 × 30 cm). The samples were loaded from the top with a metal scaffold and door was locked with metal clamps. A built-in temperature sensor was designed in the freezing chamber to monitor the temperature change and control the release of liquid nitrogen to the chamber during freezing. The programmed freezer is chamber temperature and time controlled to achieve target temperature. The freezer was programmed according to the trial experiments to control three freezing conditions namely protocol A, B and C. All the systems were programmed to prefreezing from 2 °C to target freezing temperature within a considered time followed by immediate cooled to −80 °C and held for 1 h prior to transfer to store in a chest freezer at −90 °C. The freezing profiles of each system are shown in Fig. 1. The gel temperatures during freezing were recorded at 1 s interval using type-T thermocouples (copper-constantan) connected to a data logger (Memory HiLOGGER LR8431, HIOKI E.E. Corporation, Nagano, Japan). The thermocouples (diameter 0.046 mm, response time <1 s, T-T40, Ishikawansangyo, Co. Ltd., Japan) were inserted to the center of the gels prior to freeze and attach to the aluminium plate with adhesive tape. The frozen gels were removed from the freezer and thawed at 25 °C under the ambient laboratory condition for 3 h prior to measure for mechanical properties and Raman spectra.

2.3. X-ray tomography

A Skyscan 1172 X-ray microcomputed tomography system (X-rayCT, Bruker, Kontich, Belgium) was used to measure the microstructures of freeze-dried solids which reflected ice formation in maltodextrin-agar systems. The frozen maltodextrin-agar systems were transferred to store at −90 °C for further 3 h prior to freeze-dry at below 100 Pa for approximately 60 h in a freeze-dryer (Kyowac, Kyowa Vacuum Engineering Co., Ltd., Tokyo, Japan). The vacuum was released with an ambient air. The freeze-dried solids were removed and stored in an evacuated desiccator containing P_2O_5 for 5 days to remove residual water prior to the measurement. The freeze-dried gels were wrapped with a cling film to prevent water adsorption and mounted on a rotational plate. The X-ray

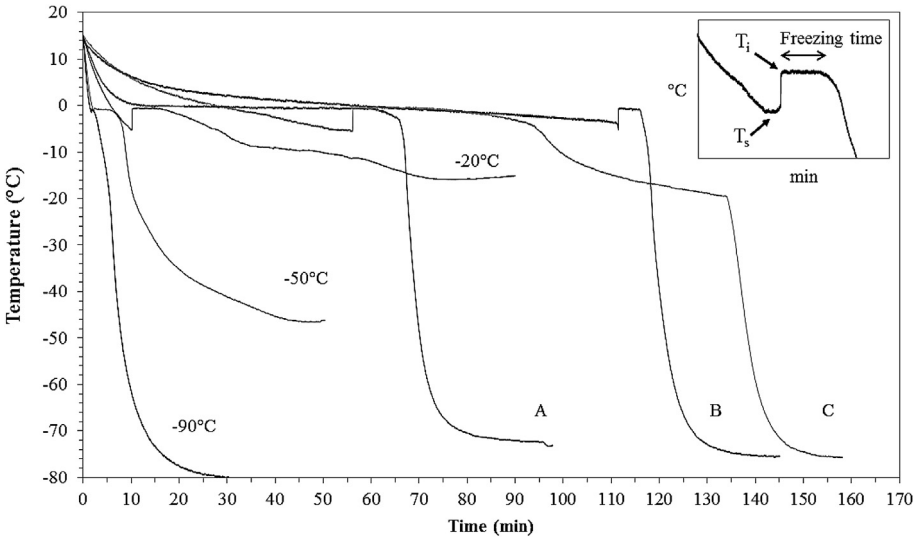

Fig. 1. Freezing profiles of maltodextrin-agar gels underwent various freezing conditions. Inlet figure shows the initial freezing point (T_i), supercooling temperature (T_s) and freezing time of a typical freezing profile. Freezing time refers to the time allows for phase transition of liquid water into ice.

voltage and current was 54 kV and 100 μA, respectively. A CCD camera with 2000 × 1332 pixels was used to record the transmission of the conical X-ray beam through all samples. The distance source-object-camera was adjusted to produce images with a pixel size of 13.59 μm. Two frames averaging, a rotation step of 0.4° with 10 random movement and an exposure time of 1840 ms were chosen to cover a view of 180° contributed to the scan time of 60 min. Three-dimensional reconstruction of samples was created by stacking of two-dimensional tomographs from a total of 800–1000 slices with a slice spacing of 0.013 mm using the reconstruction NRecon software (Version 1.6.8.0, Bruker, Kontich, Belgium). A ring artifact reduction (set to 7) and beam hardening correction (52%) were performed with NRecon software.

2.4. Mechanical properties

Mechanical properties of fresh and freeze-thawed gels were measured with a rheometer (Rheoner RE-3305, Yamaden, Co, Tokyo, Japan) equipped with a 2 N load cell. The penetration test was performed with a cylindrical plunger (diameter, 2 mm) at a speed of 0.5 mm/s and a constant deformation of 50%. The first peak force of penetration test defined as the 'hardness' which is the force required to rupture the gels and expresses as Newton (N); whereas, the 'firmness' of the gels shows the resistance to penetration and was determined from the slope of the first peak force and penetration depth reported in N/mm. The gel hardness and firmness values were calculated using data measured for 5–7 replicate samples.

2.5. Raman microscopy

Raman spectra of fresh and freeze-thawed maltodextrin-agar gels were collected using a DXR Raman microscope (Thermo Fisher Scientific, Madison, WI, USA) connected to a 100 W halogen lamp with an intensity adjustment system (TH4-100, Olympus Corporation, Tokyo, Japan). Gel specimens were placed on a microscopic glass slide and placed on the Raman microscopic stage and adjusted with a joystick controller (PROSCAN III, Prior Scientific Instruments Ltd., Cambridgeshire, UK). The samples were immediately measured after placing into the microscopic systems using a 532 nm excitation laser with 10 mW laser powers and an aperture of 50-μm pinhole at 50× microscope magnifications. The spectra were collected with 2 times of laser exposure and exposure time of 10 s. The collected spectra were baseline corrected and smoothed by using the Thermo Scientific OMNIC™ for Dispersive Raman software version 9.2.41 (Thermo Fisher Scientific, Madison, WI, USA). All data were collected and reported as Raman shifts within the range from 3500 to 100 cm^{-1}.

2.6. Micro differential scanning calorimetry (μDSC)

The phase transitions temperatures namely glass transition temperature (T_g) and onset temperature of ice melting (T_m') were determined using a micro differential scanning calorimetry (μDSC VII Evo, SETARAM, KEP Instrumentation, Caluire, France). Approximately 80–90 mg of maltodextrin-agar gels were transferred into a standard hastelloy DSC cell. Duplicate samples were scanned within the range of −45 °C to 20 °C at a rate of 1 °C/min. The thermal properties were derived from the onset temperature of the heating scan using the Calisto software (Version 1.14, SETARAM, KEP Instrumentation, Caluire, France).

2.7. Statistical analysis

The parameters derived from Raman spectra (peak height, peak area and full width at half height; FWHH) centered at 480 cm^{-1} were subjected to analysis of variance (ANOVA). Duncan's multiple range test at 95% confidence intervals were carried out for mean comparison using SPSS 17.0 software for Windows (SPSS Inc., Chicago, USA). The differences between maltodextrin DEs and freezing conditions were analyzed.

3. Results

3.1. Freezing properties

Gel systems contained maltodextrin at various DEs (DE5, DE15 and DE18) were frozen at various freezing conditions composed of chest freezers (−20 °C, −50 °C and −90 °C) and controlled freezing (protocol A, B and C). The freezing profile and properties of gels containing maltodextrin DE15 are shown in Fig. 1 and Table 1, respectively. The freezing properties were determined from the

Table 1
Freezing properties; cooling rate, supercooling temperature (T_s), initial freezing point (T_i) and freezing time of agar gels containing maltodextrin underwent various freezing conditions namely conventional freezing temperature of −20 °C, −50 °C and −90 °C, and controlled freezing protocol A, B and C.

Freezing protocol	Cooling rate[a] (°C/min)	T_s (°C)	T_i (°C)	Freezing time (min)
−20 °C	1.04 ± 0.18	−8.1 ± 2.9	−0.6 ± 0.1	4 ± 2
−50 °C	2.18 ± 0.81	−1.0 ± 0.2	−0.6 ± 0.3	5 ± 0
−90 °C	3.84 ± 0.12	−1.6 ± 0.1	−1.1 ± 0.2	1 ± 1
A	0.02 ± 0.00	N/A	−0.2 ± 0.0	40 ± 3
B	0.08 ± 0.00	−3.7 ± 0.1	−0.4 ± 0.0	3 ± 0
C	0.17 ± 0.01	−5.2 ± 0.2	−0.6 ± 0.1	30 ± 3

Values shown are mean ± SD (n = 3).
[a] Cooling rates were derived from the initial slope of the freezing profile.

freezing profile as shown in Fig. 1. The initial slope was calculated as cooling rate of the systems; whereas the freezing time refers to the period of which the liquid water transformed into ice. Table 1 shows that the decrease of freezer temperature resulted in a faster cooling rate ($p \leq 0.05$), lower initial freezing temperature (T_i) and reduced freezing time (time between T_i and the drop of temperature from the freezing plateau as shown in Fig. 1) which reflected the time for the ice growth. The results showed that the supercooling temperature (T_s) of maltodextrin systems can possibly be less than −1.0 °C to −8.1 °C.

Fig. 1 clearly indicated that the initial cooling rate (slope of cooling curve) of protocol A at above 2 °C was around 1.0 °C/min, and thereafter sharply decreased when the temperature was 0 °C. The initial fast cooling caused the temperature gradient within gel matrices and surface temperature was lower than the core temperature. The ice nucleation possibly took place at the surface resulting in the release of latent heat. The slow cooling rate of the chamber (0.17 °C/min) cannot extract the heat of crystallization which raised the matrices temperature and, therefore, the nucleation proceeded with a slower cooling rate of 0.02 °C/min. It is presumed that an extremely slow ice nucleation took place and was followed by a long freezing time and hence ice growth. Freezing protocol B was programmed to achieve a slow cooling rate (0.08 °C/min) and in the supercooled region (subzero temperature, < 0 °C) where ice has not yet formed, the temperature was programmed to drop immediately by quench cooling to −80 °C. Consequently, the releases of latent heat of crystallization were observed in all DE systems followed by a very limited freezing time due to a rapid quenching of chamber temperature to −80 °C. Freezing protocol B represented slow cooling followed by a very rapid freezing condition; whereas, the ice crystallization in protocol C were completed with a constant cooling and freezing rate of 0.17 °C/min. Such constant freezing rate was identical to that generally obtain in conventional freezers.

The μDSC showed the onset of ice melting temperature for maltodextrin-agar gels with DE5, DE15 and DE18 as −10 °C, −18 °C and −18 °C, respectively (Fig. 2). The thermograms indicated that all the DEs systems were kept frozen below the onset temperature of ice melting or T_m' at which the maximum ice formed in the matrices. The difference molecular weight of DE15 and DE18 systems showed similar DSC thermal properties. High molecular weight polymer including starch and maltodextrin show a very small endothermic shift of heat flow indicating glass transition temperature (T_g) that is very difficult to detect with a DSC. However, the μDSC in the present study clearly revealed an endothermic shift of heat flow of maltodextrin DE5 and DE15 systems suggesting T_g at −19 °C and −30 °C, respectively. The results confirmed that increased small molecular weight components led to a decreased T_g of the gel systems.

3.2. Microstructures

The x-ray CT images of freeze-dried solids reflected the ice formation during freezing of maltodextrin systems (Figs. 3 and 4).

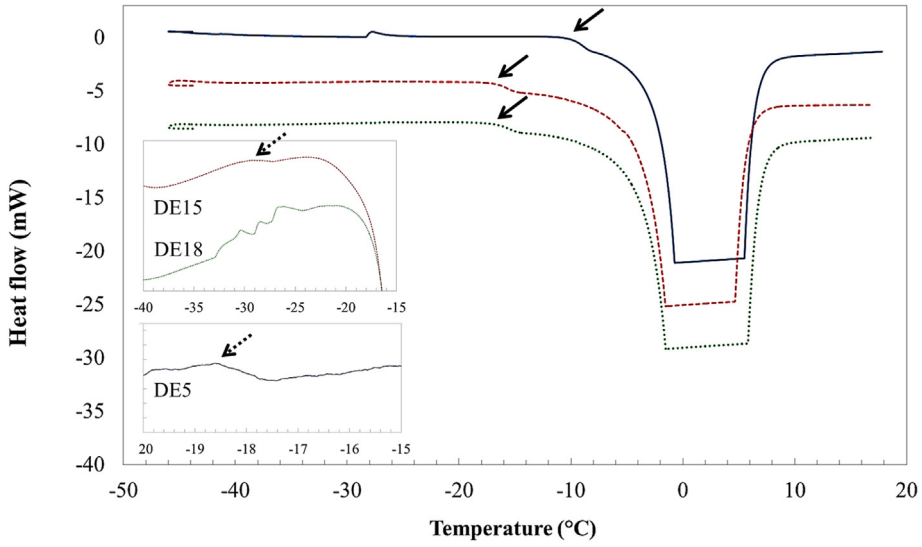

Fig. 2. DSC thermograms of agar gels containing maltodextrin (DE5, DE15 and DE18). Arrows indicate onset of ice melting temperature (T_m'). Inlet figures are zoomed in DSC thermograms with arrows showing the endothermic shift of heat flow refers to glass transition temperature (T_g) of the systems. Full (—), dash (–) and dotted (···) line indicate DE5, DE15 and DE18 systems, respectively. Full and dotted arrows indicate T_m' and T_g of the gels, respectively.

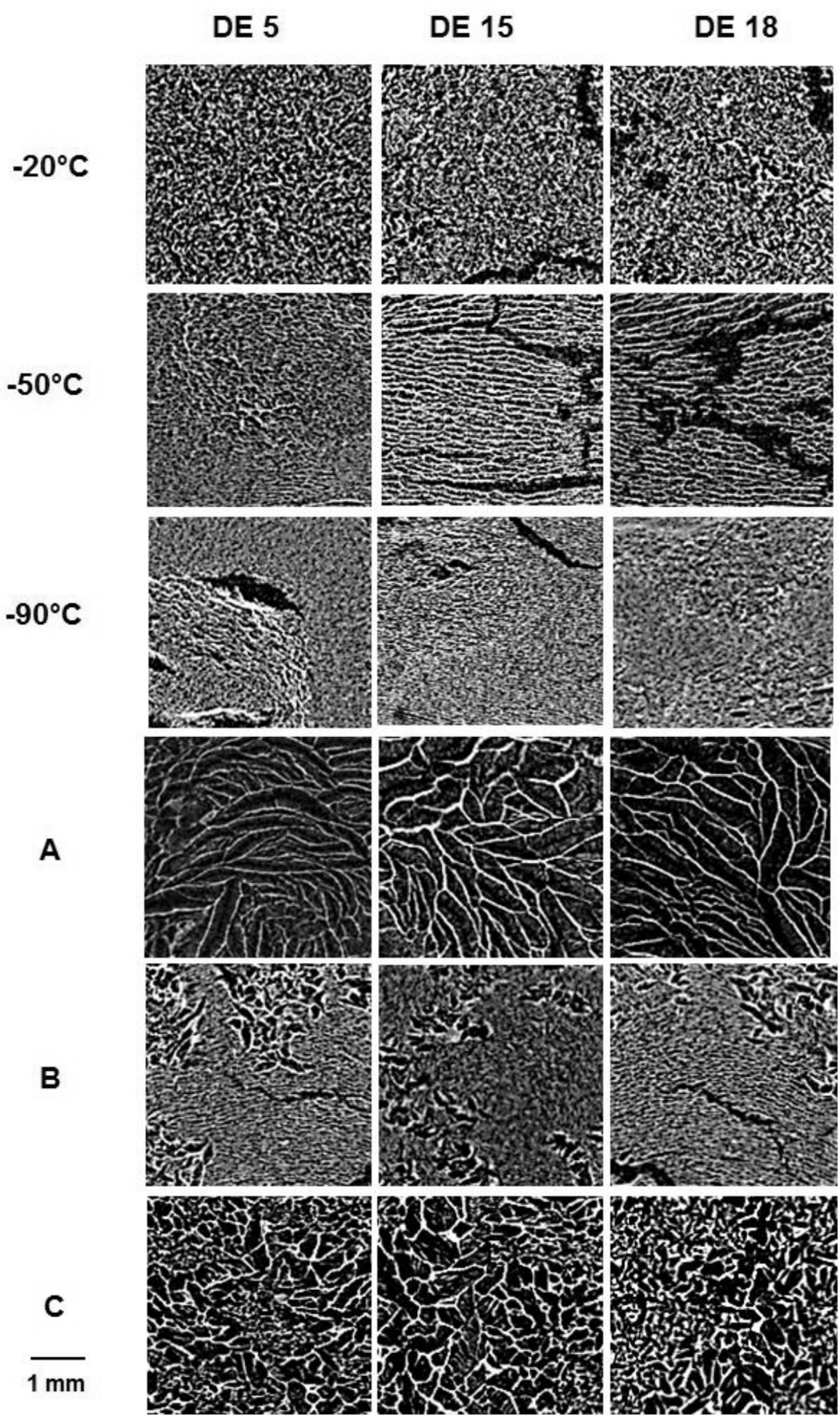

Fig. 3. Cross sectioned images of freeze-dried gels containing maltodextrin (DE5, DE15 and DE18) underwent various freezing conditions (freezing temperature of −20 °C, −50 °C and −90 °C, and controlled freezing protocol A, B and C). Dark region indicates void spaces of freeze-dried matrics reflecting ice morphology formed during freezing embeded in solid network.

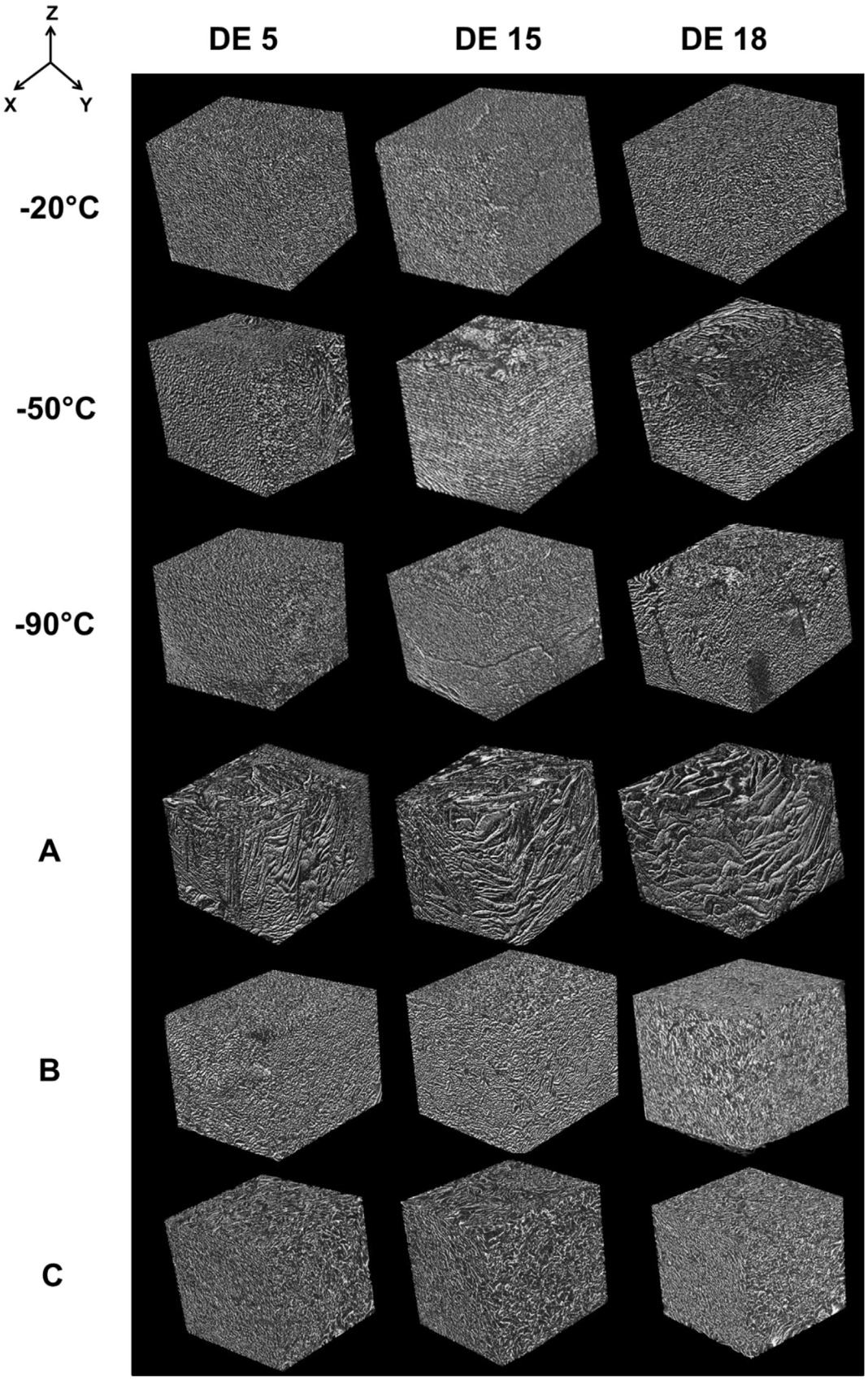

Fig. 4. X-ray CT images showing 3D structures of freeze-dried gels containing maltodextrin (DE5, DE15 and DE18) underwent various freezing conditions (freezing temperature of −20 °C, −50 °C and −90 °C, and controlled freezing protocol A, B and C).

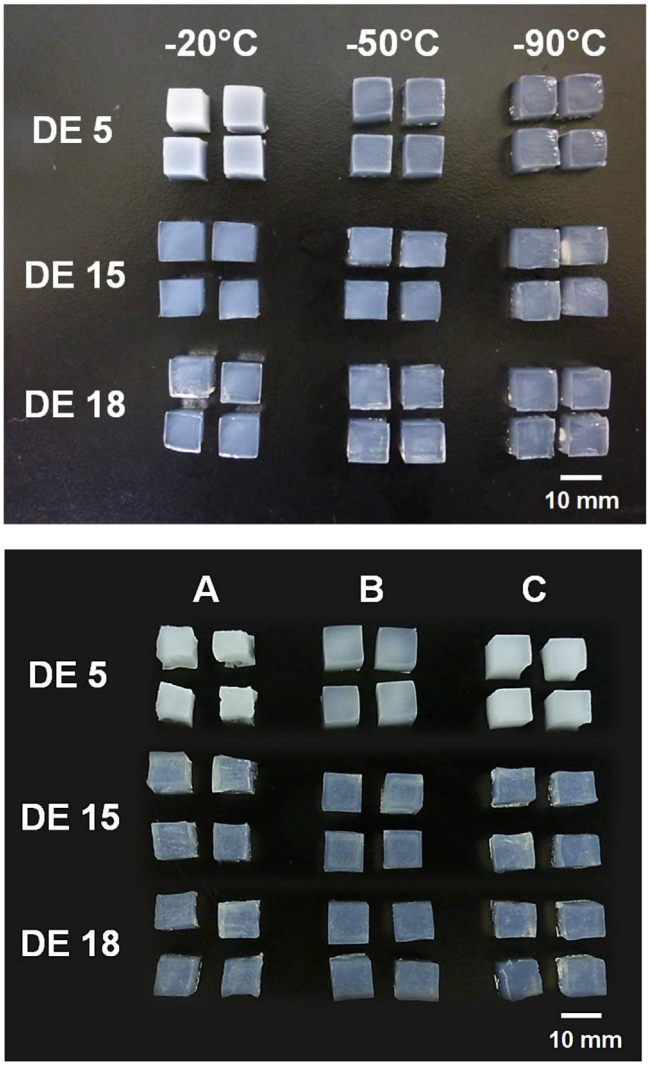

Fig. 5. Appearance of thawed agar gels containing maltodextrin of various dextrose equivalents (DE5, DE15 and DE18) at 25 °C for 3 h underwent various freezing conditions (freezing temperature of −20 °C, −50 °C and −90 °C, and controlled freezing protocol A, B and C) suggesting shrinkage and turbidity after freeze-thawing.

increased the ice growth resulting in a large size of ice crystal formation. Conversely, the extremely slow cooling rate caused slow nucleation and an extended ice growth period suggested by a long freezing time which formed large dendritic ice crystals in the freezing protocol A (Fig. 1 and Table 1). Interestingly, a slow cooling to a supercooled region (~0 °C to −1 °C) followed by a rapid quench cooling (to −80 °C) induced nucleation possibly by the temperature fluctuation followed by a very limited freezing time in protocol B. The frozen structures with a few irregular shaped large ice crystals surrounded by small ice crystals embedded in gel matrix were formed. The slow cooling rate of −20 °C, and protocol B and C systems led to a lower supercooled temperature without ice crystallization. The result is important to the freezing of food products with a larger size where a homogeneous cooling of the bulk matrices is required before the ice formation to achieve more homogeneous freezing and hence ice morphology. The results showed that a slow cooling of such products to a supercooled region to achieve a homogeneous temperature followed by a very rapid cooling can mainly form small ice crystals. The quench cooling after achieving nucleation effectively limited crystal growth and, therefore, small ice crystals sizes were formed. A slow freezing with undercooling produced non-homogeneous of small and large ice crystals embedded in gel matrix in accordance with Charoenrein and Preechathammawong (2010). A faster cooling rate and hence faster nucleation was achieved in protocol C; however, a longer period of crystal growth caused the formation of larger ice crystals (Harnkarnsujarit et al., 2012). The diverse molecular size of maltodextrin in the presence study, however, showed an unclear difference of the gel microstructures due to a low contrast and magnification of the image (Figs. 3 and 4).

3.3. Shrinkage and turbidity

The appearance of freeze-thawed gels is shown in Fig. 5. The freezing protocol A clearly caused shrinkage upon thawing which was coincident with the large hole embedded in thick aggregated gel matrices. A slightly less shrinkage was also observed in protocol C which had a smaller size of ice formed in matrices. Conversely, the small size of ice crystals formed in protocol B and freezing conditions at −20 °C, −50 °C and −90 °C effectively retained high gel network connectivity and resulting in no shrinkage structure. Although protocol B had inhomogeneity structures, the gel network was strong enough to prevent structural shrinkage. Upon thawing, the liquid water was expelled leaving pores embedded in the gel network. The network of amorphous solid provides mechanical strength against gravimetric and capillary force which accelerated and causes structural collapse (Rahman, 2001). The least solid connectivity of protocol A gave least mechanical strength and hence the highest degree of structural shrinkage.

Table 2
Mechanical properties (hardness and firmness) of unfrozen and freeze-thawed gels containing maltodextrin of various dextrose equivalents (DE5, DE15 and DE18) underwent various freezing conditions (freezing temperature of −20 °C, −50 °C and −90 °C, and controlled freezing protocol A, B and C).

Mechanical property	Gel system	Unfrozen	Freezing protocols					
			−20 °C	−50 °C	−90 °C	A	B	C
Hardness (N)	DE 5	0.821 ± 0.238	0.157 ± 0.017	0.118 ± 0.028	0.165 ± 0.025	0.223 ± 0.052	0.156 ± 0.022	0.133 ± 0.033
	DE 15	0.883 ± 0.252	0.141 ± 0.042	0.154 ± 0.035	0.190 ± 0.027	0.209 ± 0.049	0.174 ± 0.016	0.142 ± 0.021
	DE 18	0.940 ± 0.268	0.154 ± 0.048	0.196 ± 0.017	0.239 ± 0.009	0.209 ± 0.037	0.174 ± 0.015	0.125 ± 0.023
Firmness (N/mm)	DE 5	0.036 ± 0.011	0.055 ± 0.007	0.036 ± 0.006	0.050 ± 0.007	0.026 ± 0.007	0.038 ± 0.007	0.023 ± 0.005
	DE 15	0.078 ± 0.016	0.037 ± 0.013	0.046 ± 0.010	0.053 ± 0.014	0.043 ± 0.014	0.038 ± 0.010	0.029 ± 0.003
	DE 18	0.059 ± 0.011	0.038 ± 0.010	0.062 ± 0.008	0.073 ± 0.007	0.038 ± 0.007	0.047 ± 0.002	0.029 ± 0.003

Values shown are mean ± SD (n = 5 to 7).

The decreased freezer temperature and hence a faster cooling rate gave a faster nucleation and limited time allowed for the ice growth contributed to formation of a high number of small ice crystals. Regardless of conventional and controlled freezing conditions, a rapid cooling rate as determined by the initial slope of the cooling curve enhanced formation of many small ice crystals; whereas, a longer freezing time as suggested by the plateau after supercooling

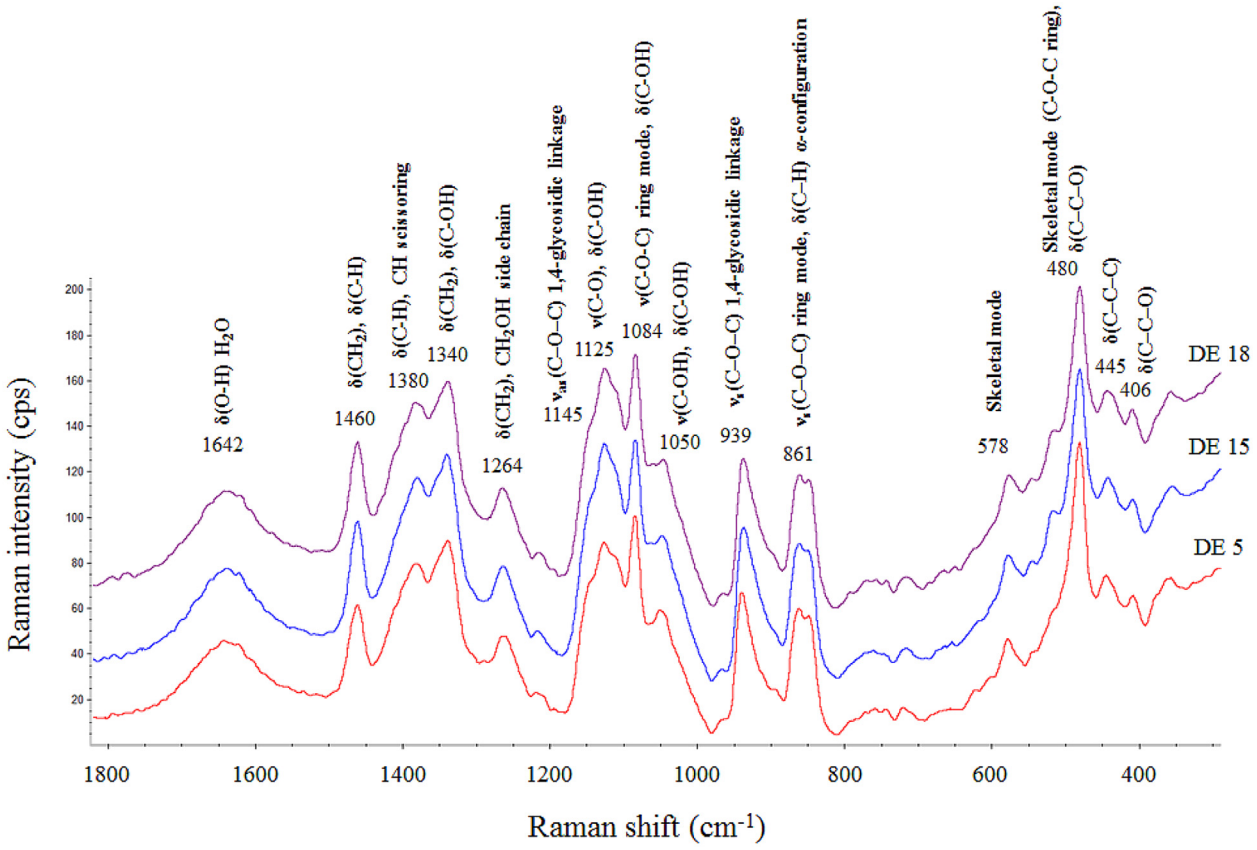

Fig. 6. Raman spectra showing the position (cm^{-1}) and assignments of agar-maltodextrin gels with different dextrose equivanlent (DE5, DE15 and DE18) of maltodextrin. The band assignments were from Cael, Koenig, and Blackwell (1973), Bulkin et al. (1987), Sekkal, Dincq, Legrand, and Huvenne (1995); Schuster et al. (2000) and Pigorsch (2009).

Upon thawing, turbidity of the gels was clearly observed in DE 5 systems frozen at −20 °C (Fig. 5). The systems frozen at −50 °C showed only slight turbidity on the edge; whereas, clear gels were observed for systems frozen at −90 °C. The DE15 and DE18 showed no turbidity at all freezing temperatures. In case of program freezing, the DE5 systems underwent freezing protocol A had the highest turbidity followed by protocol C; whereas protocol B showed only slight turbidity.

3.4. Mechanical properties

The hardness and firmness values of the freeze-thawed gels are shown in Table 2. The results clearly showed that increased DE of maltodextrin gave an increased mechanical strength (hardness and firmness) of the fresh gel systems. Sworn and Kasapis (1998) showed the effects of co-solute types and concentrations on mechanical strength of gellan gel that 14-DE of maltodextrin had less firmness than 42-DE of corn syrup up to 40 g/100 g. The lower DE of solids contained higher fraction of large molecular weight components which possibly hindered the association of agarose chain to form helix structures resulting lower mechanical strength than high DE systems.

The mechanical strength of all DE systems decreased sharply upon freeze-thawing in agreement with Kozłowicz and Kluza (2012). Freezing causes phase separation of ice and solutes and accelerated irreversible aggregation of junction network. Lower temperature freezing had a slightly higher mechanical strength (hardness and firmness) than higher temperature freezing because of less modification of junction networks due to freezing. It is also presumed that smaller molecular weight solutes (higher DE) increased amount of unfrozen water and, therefore, less ice formed than low DE systems leading to less structural disintegrity induced by ice formation contributed to a higher strength in higher DE systems frozen at −20 °C, −50 °C and −90 °C.

However, DE showed insignificant effects on mechanical strength of systems frozen by programmed freezing. Freezing protocol A gave high degree of gel shrinkage upon thawing resulted in a high hardness values which was independent of the DE of maltodextrin. A drop of the firmness values of DE5 frozen by protocol A and C was observed in concurrent with the shrinkage and turbidity of the thawed gels. Low temperature freezing formed small size of ice crystals and hence higher integrity of the gel networks resulting in a higher mechanical strength; however, the DE5 systems frozen at −20 °C which had non-shrinkage showed a higher firmness than −50 °C and −90 °C systems in concurrent with a high turbidity.

A thicker size of gel network formed in concurrent with large ice crystal sizes (protocol A and C) decreased mechanical strength and accelerated shrinkage of the gels upon thawing (Fig. 3 and Table 2). Thawed gels frozen by protocol A had high degree of collapsed network which increased the strength against penetration force resulting in the highest hardness in all DE systems (Table 2). Fig. 3 clearly shows that decreased freezer temperature from −20 °C to −90 °C formed a smaller size of ice and thinner solid networks with a higher connectivity. Consequently, the decreased freezer temperature formed a closer proximity of solid network resulted in a higher mechanical strength of thawed gels.

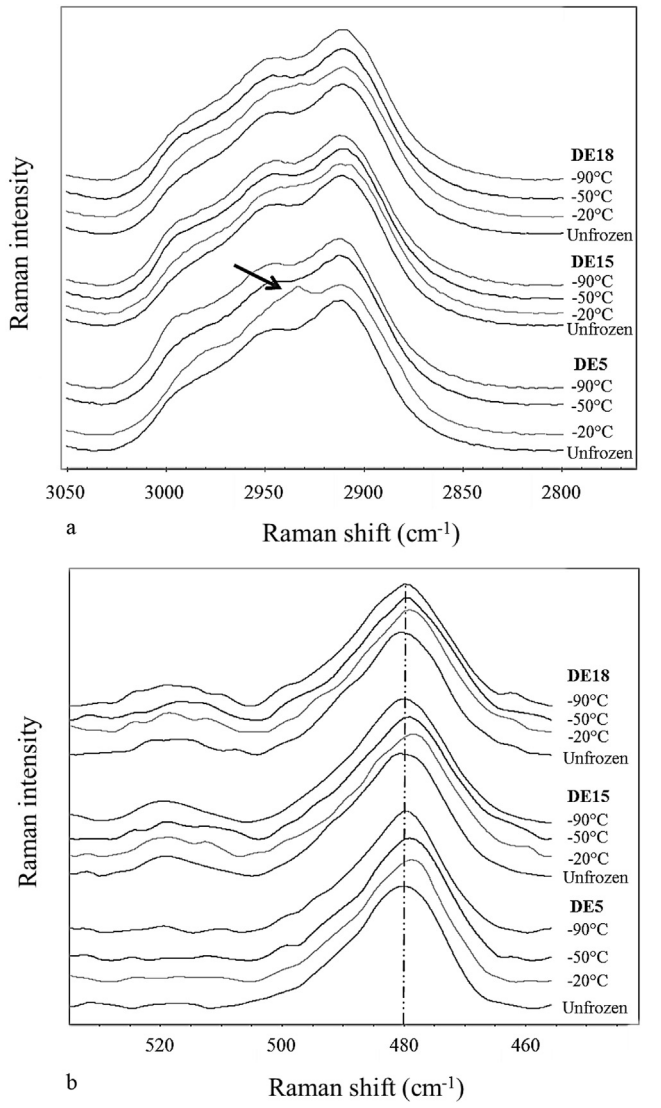

Fig. 7. Raman spectra of unfrozen and freeze-thawed maltodextrin-agar gels at various freezing temperatures (−20 °C, −50 °C and −90 °C) in the region of (a) 2800–3050 cm^{-1} and (b) 450–550 cm^{-1}. Arrows indicates a clear developed peak after freezing at −20 °C of DE5 system.

3.5. Recrystallization of maltodextrin-agar gels upon thawing

The Raman spectra of maltodextrin-agar gels and their vibration modes are shown in Fig. 6. The results agreed well to the Raman spectra of starch and amylose/amylopectin reported by previous researchers (Bulkin et al., 1987; Cael, Koenig, & Blackwell, 1975; De Veij, Vandenabeele, De Beer, Remon, & Moens, 2009; Łabanowska, Wesełucha-Birczyńska, Kurdziel, & Sepioło, 2013). The Raman bands for different DE systems were similar. However, the increased degree of polymerization (lower DE) resulted in a stronger band at 1050 cm^{-1} assigned to stretching (ν) and bending (δ) vibration of C–O–H bonds as well as a broader band at 480 cm^{-1}. After freeze-thawing, the Raman spectra revealed structural changes in the region between 2800 and 3050 cm^{-1} and 450–550 cm^{-1} (Fig. 7a and b) which were assigned to νC-H stretching vibration and skeletal modes of pyranose ring, respectively (Bulkin et al., 1987; Tu, 1982). In the νC-H stretching region, the major peak located at 2910 cm^{-1} due to symmetric stretching of νCH_2 with overlapped shoulders around 2950 and 3000 cm^{-1} assigned for assymetric νCH_2 and νC-H stretching, respectively (Łabanowska et al., 2013). The freezing at −20 °C introduced an emerged peak at 2930 cm^{-1}, particularly, in DE5 systems. The results showed the structural changes associated with C–H structures.

Freezing obviously revealed impact on Raman peak centered at 480 cm^{-1} namely the shift of band maximum and shape of the band. Fig. 8 shows a significant shift to a lower wavenumber of band maximum at 480 cm^{-1} in all DE systems frozen at −20 °C and −50 °C compared to unfrozen systems. Moreover, the band narrowing and hence decreased full width at half height (FWHH) was clearly observed in DE 5 systems after freeze-thawing (Table 3). Nevertheless, the freezing conditions revealed insignificant effects on the band width. The DE 15 and DE 18 showed slightly decreased FWHH; whereas freezing showed an unclear effect on band narrowing of DE 15 and DE 18 systems possibly due to less amounts of high molecular weight components. The DE 15 and DE 18 systems had a lower peak height and peak area than DE 5 system. Freezing reduced the peak height and peak area in all DE systems which indicated the structural changes of the gel components due to freezing. The fast freezing at −90 °C, however, showed no effects on peak height of DE 18 systems.

The drastic shift and narrowing of the bands at 480 cm^{-1} suggested significant amorphous–crystalline transition of DE 5 systems. Fechner et al. (2005) found that a slight shift of approximately 1–2 cm^{-1} of the Raman maximum at 480 cm^{-1} was coincident

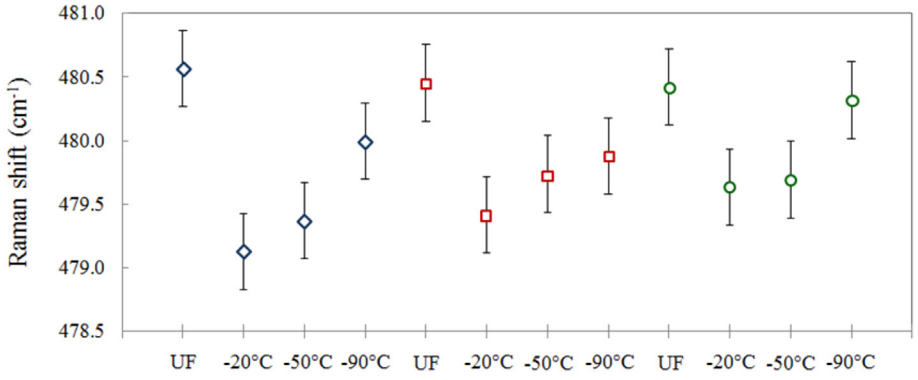

Fig. 8. Raman shift number and full width at half height (FWHH) of the band maximum at 480 cm^{-1} of unfrozen (UF) and freeze-thawed maltodextrin-agar gels namely DE5 (◊), DE15 (□) and DE18 (○) maltodextrin underwent various freezing temperatures (−20 °C, −50 °C and −90 °C). Values shown are mean and error bars indicate standard deviation (n = 23).

Table 3
Raman spectra analysis namely peak height, full width at half-height (FWHH) and peak area of band centered at wavenumber of 480 cm^{-1} of unfrozen and freeze-thaw agar-maltodextrin gels at various dextrose equivalents (DE5, DE15 and DE18).

System	Peak height				FWHH				Peak area			
	Unfrozen	Freezing			Unfrozen	Freezing			Unfrozen	Freezing		
		−20 °C	−50 °C	−90 °C		−20 °C	−50 °C	−90 °C		−20 °C	−50 °C	−90 °C
DE5	109.9 ± 18.9 aA	88.0 ± 18.2bA	98.0 ± 10.4bA	74.5 ± 7.6 cA	25.6 ± 2.7 aA	22.3 ± 3.7bB	24.6 ± 2.4abA	22.6 ± 4.5bA	5185.5 ± 1193.1 aA	2875.2 ± 1542.8 cA	4312.6 ± 833.5bA	2863.7 ± 1344.5 cA
DE15	75.8 ± 8.3 aB	56.7 ± 6.6 cC	59.2 ± 4.9 cB	63.8 ± 7.8bB	23.8 ± 2.8bB	27.7 ± 3.9 aA	21.6 ± 2.9bB	24.4 ± 9.7bA	2841.4 ± 808.5 aB	2953.8 ± 1155.5 aA	1889.2 ± 627.7bB	1775.8 ± 1565.9bB
DE18	79.7 ± 8.6 aB	65.8 ± 6.8bB	57.8 ± 9.4 cB	74.5 ± 10.4 aA	22.3 ± 2.2bB	22.8 ± 4.2bB	26.1 ± 6.6 aA	21.4 ± 4.4bA	2799.3 ± 885.5 aB	2160.5 ± 1475.1 aA	2377.0 ± 1227.2 aB	1251.1 ± 1186.7bB

Different lower case letters indicate significant difference ($p \leq 0.05$) in the same column.
Different upper case letters indicate significant difference ($p \leq 0.05$) in the same row.

with the recrystallization of starch in gel systems which includes helix formation and helix–helix aggregation. The shift of the band maximum at 480 cm^{-1} and band narrowing in freeze-thawed gels suggests the recrystallization of starch-like components in maltodextrin, particularly amylose recrystallization which occur within a few hours (Fechner et al., 2005). The initial disorder state of starch-like components in maltodextrin systems has a range of molecular conformations; however, systems became more ordered upon recrystallization. Consequently, the number of conformations decreased leading to a smaller distribution of bond energies compared with the initial state and hence the Raman band narrowing was observed (Karim et al., 2000; Van Soest, De Wit, Tournois, & Vliegenthart, 1994). The results indicated the highest degree of maltodextrin recrystallization in systems frozen −20 °C followed by −50 °C systems. Moreover, the maltodextrin recrystallization was more pronounced in lower DE systems which attributed to a higher degree of polymerization of starch-like polymers. Conversely, the gels prefrozen at −90 °C showed similar Raman spectra to the unfrozen systems and insignificant decreased wavenumbers was observed which suggest efficacy to maintain molecular structure of carbohydrate components.

The results indicated that large pore size in concurrent with thicker network in low DE solids decreased strength of gel network; however, a high firmness was observed in DE 5 system frozen at −20 °C which was coincident with the gel turbidity developed during thawing. The turbidity of the matrices suggested the recrystallization of starch-like components (Karim et al., 2000) which confirmed by the shift and narrowing of the Raman spectra around 450–550 cm^{-1} and the changes associated to νC-H stretching region (Figs. 7b and 8). The DE 5 system had least degree of starch hydrolysis and hence higher content of starch polymer; therefore, the amorphous–crystalline transition or recrystallization of starch possibly took place upon cooling and thawing contributed to the turbidity of the gels. The amylose and amylopectin recrystallizations at low temperature have been demonstrated by previous researches, particularly, in starch-based systems which contributed to changes of mechanical properties i.e. increased firmness of starch gel systems (Miles, Morris, Orford, & Ring, 1985). Kim and Lee (1987) also observed an increased penetration force associated with the increased recrystallization of starch components in surimi gels. The recrystallization has been reported to increased firmness of starch-based systems ex. bread, rice and gel systems (Kim & Lee, 1987; Morgan, Gerrard, Every, Ross, & Gilpin, 1997; Perdon, Siebenmorgen, Buescher, & Gbur, 1999; Seow & Teo, 1996). Consequently, the unexpected increased mechanical strength of DE 5 system frozen at −20 °C attributed to the recrystallization of starch components.

Fig. 5a clearly showed that a low temperature freezing and corresponding faster freezing resulted in a slower recrystallization rate than slower freezing systems. The small ice crystals caused a quicker thawing and gels subsequently pass through the temperature of maximum recrystallization faster than slow frozen systems which minimized starch recrystallization (Yu, Ma, & Sun, 2010). Rapid freezing resulted in less structural changes of starch-based foods including recrystallization of starch components than slow freezing (Kock, Minnaar, Berry, & Taylor, 1995; Ma & Sun; 2009; Navarro, Martino, & Zaritzky, 1995).

The cooling period of protocol B was longer than A and C (Fig. 1) suggested a longer exposure to maximum recrystallization temperature; however, the DE5 gels showed less turbid (Fig. 5). Moreover, all the frozen storage temperature was lower than the T_g of the DE5 gels (Fig. 2). The gels were considered to be in the glassy state which possibly restricted the molecular mobility and hence recrystallization of the gels (Goff, 1992). This confirmed that the recrystallization of maltodextrin components primarily took place

during thawing and is accelerated by ice crystallization that modified microstructures of food matrices. The DE5 systems frozen by protocol A had the highest turbid followed by protocol C, −20 °C, protocol B and −50 °C, respectively. This order of starch recrystallization was in agreement with the thickness of solid network form after freezing as shown in Fig. 3. Therefore, physical aggregation of solid network possibly enhanced intermolecular association and accelerated starch recrystallization. In addition, the highest turbidity of DE5 frozen by protocol A was coincided with the highest degree of structural shrinkage and least firmness values (Fig. 5). It is presumed that the drastic recrystallization of starch components caused phase separation between crystalline and amorphous solids that decreased mechanical strength which accelerated gel shrinkage.

4. Conclusions

The results showed that freezing affected gel microstructure, mechanical strength and subsequent structural changes of thawed solid gels. The X-ray CT images reflected the size and morphology of ice crystals formed during freezing and determined microstructures of frozen agar-maltodextrin gels. Freezing also modified gel structures as shown by the changes of the Raman spectra. The band shift and narrowing at 480 cm^{-1} assigned to skeletal modes of pyranose ring suggested amorphous–crystalline transition of maltodextrin components in concurrent with the increased turbidity of low DE systems after freeze-thawing. Large pores embedded in thicker solid networks accelerated gel shrinkage which was independent of freezing rate. The recrystallization of the gel components initially increased mechanical strength; however, further accelerated shrinkage of matrices possibly due to the phase separation between crystalline and amorphous phases. The ice crystallization controlled microstructures of solids (pore and membrane thickness) which influenced shrinkage and recrystallization upon thawing.

Acknowledgment

The authors gratefully acknowledge the Ministry of Education, Culture, Sports, Science and Technology of Japan on the project title of “MEXT Revitalization Project for the creation of Fisheries Research and Education Center in Sanriku” for the financial support.

References

Badii, F., & Howell, N. K. (2002). Changes in the texture and structure of cod and haddock fillets during frozen storage. *Food Hydrocolloids, 16*(4), 313–319.
Benjakul, S., Visessanguan, W., Thongkaew, C., & Tanaka, M. (2003). Comparative study on physicochemical changes of muscle proteins from some tropical fish during frozen storage. *Food Research International, 36*(8), 787–795.
Bulkin, B. J., Kwak, Y., & Dea, I. (1987). Recrystallization kinetics of waxy-corn and potato starches; a rapid, Raman-spectroscopic study. *Carbohydrate Research, 160*, 95–112.
Cael, S. J., Koenig, J. L., & Blackwell, J. (1973). Infrared and raman spectroscopy of carbohydrates: Part III: Raman spectra of the polymorphic forms of amylose. *Carbohydrate Research, 29*(1), 123–134.
Cael, J. J., Koenig, J. L., & Blackwell, J. (1975). Infrared and Raman spectroscopy of carbohydrates. Part VI: normal coordinate analysis of V-amylose. *Biopolymers, 14*(9), 1885–1903.
Charoenrein, S., & Preechathammawong, N. (2010). Undercooling associated with slow freezing and its influence on the microstructure and properties of rice starch gels. *Journal of Food Engineering, 100*(2), 310–314.
Chronakis, I. S. (1998). On the molecular characteristics, compositional properties, and structural-functional mechanisms of maltodextrins: a review. *Critical Reviews in Food Science and Nutrition, 38*(7), 599–637.
De Veij, M., Vandenabeele, P., De Beer, T., Remon, J. P., & Moens, L. (2009). Reference database of Raman spectra of pharmaceutical excipients. *Journal of Raman Spectroscopy, 40*(3), 297–307.
Fechner, P. M., Wartewig, S., Kleinebudde, P., & Neubert, R. H. (2005). Studies of the recrystallization process for various starch gels using Raman spectroscopy. *Carbohydrate Research, 340*(16), 2563–2568.
Gibbs, F., Kermasha, S., Alli, I., Catherine, N., & Mulligan, B. (1999). Encapsulation in the food industry: a review. *International Journal of Food Sciences and Nutrition, 50*(3), 213–224.
Goff, H. D. (1992). Low-temperature stability and the glassy state in frozen foods. *Food Research International, 25*(4), 317–325.
Goff, H. D. (1995). The use of thermal analysis in the development of a better understanding of frozen food stability. *Pure and Applied Chemistry, 67*(11), 1801–1808.
Harnkarnsujarit, N., Charoenrein, S., & Roos, Y. H. (2012). Microstructure formation of maltodextrin and sugar matrices in freeze-dried systems. *Carbohydrate Polymers, 88*(2), 734–742.
Karim, A. A., Norziah, M. H., & Seow, C. C. (2000). Methods for the study of starch recrystallization. *Food Chemistry, 71*(1), 9–36.
Kidmose, U., & Martens, H. J. (1999). Changes in texture, microstructure and nutritional quality of carrot slices during blanching and freezing. *Journal of the Science of Food and Agriculture, 79*(12), 1747–1753.
Kim, J. O., Kim, W. S., & Shin, M. S. (1997). A comparative study on retrogradation of Rice starch gels by DSC, X-Ray and α-Amylase methods. *Starch-Stärke, 49*(2), 71–75.
Kim, J. M., & Lee, C. M. (1987). Effect of starch of textural properties of surimi gel. *Journal of Food Science, 52*(3), 722–725.
Kock, S., Minnaar, A., Berry, D., & Taylor, J. R. N. (1995). The effect of freezing rate on the quality of cellular and non-cellular par-cooked starchy convenience foods. *Lebensmittel-Wissenschaft und-Technologie, 28*(1), 87–95.
Kozłowicz, K., & Kluza, F. (2012). Gel products properties influenced by freezing in different conditions. *International Journal of Refrigeration, 35*(6), 1715–1721.
Łabanowska, M., Wesełucha-Birczyńska, A., Kurdziel, M., & Sepioło, K. (2013). The mechanism of thermal activated radical formation in potato starch studied by electron paramagnetic resonance and Raman spectroscopies. *Carbohydrate Polymers, 91*(1), 339–347.
Lee, M. H., Baek, M. H., Cha, D. S., Park, H. J., & Lim, S. T. (2002). Freeze–thaw stabilization of sweet potato starch gel by polysaccharide gums. *Food Hydrocolloids, 16*(4), 345–352.
Li-Chan, E. C. Y. (1996). The applications of Raman spectroscopy in food science. *Trends in Food Science & Technology, 7*(11), 361–370.
Mackie, I. M. (1993). The effects of freezing on flesh proteins. *Food Reviews International, 9*(4), 575–610.
Ma, Y., & Sun, D. W. (2009). Hardness of cooked rice as affected by varieties, cooling methods and chill storage. *Journal of Food Process Engineering, 32*(2), 161–176.
Miles, M. J., Morris, V. J., Orford, P. D., & Ring, S. G. (1985). The roles of amylose and amylopectin in the gelation and recrystallization of starch. *Carbohydrate Research, 135*(2), 271–281.
Morgan, K. R., Gerrard, J., Every, D., Ross, M., & Gilpin, M. (1997). Staling in starch breads: the effect of Antistaling α-Amylase. *Starch-Stärke, 49*(2), 54–59.
Muadklay, J., & Charoenrein, S. (2008). Effects of hydrocolloids and freezing rates on freeze–thaw stability of tapioca starch gels. *Food Hydrocolloids, 22*(7), 1268–1272.
Navarro, A. S., Martino, M. N., & Zaritzky, N. E. (1995). Effect of freezing rate on the rheological behaviour of systems based on starch and lipid phase. *Journal of Food Engineering, 26*(4), 481–495.
Ngapo, T. M., Babare, I. H., Reynolds, J., & Mawson, R. F. (1999). Freezing and thawing rate effects on drip loss from samples of pork. *Meat Science, 53*(3), 149–158.
Perdon, A. A., Siebenmorgen, T. J., Buescher, R. W., & Gbur, E. E. (1999). Starch recrystallization and texture of cooked milled rice during storage. *Journal of Food Science, 64*(5), 828–832.
Petzold, G., & Aguilera, J. M. (2009). Ice morphology: fundamentals and technological applications in foods. *Food Biophysics, 4*(4), 378–396.
Pigorsch, E. (2009). Spectroscopic characterisation of cationic quaternary ammonium starches. *Starch-Stärke, 61*(3-4), 129–138.
Rahman, M. S. (2001). Toward prediction of porosity in foods during drying: a brief review. *Drying Technology, 19*(1), 1–13.
Rojas, J. A., Rosell, C. M., & de Barber, C. B. (2001). Role of maltodextrins in the staling of starch gels. *European Food Research and Technology, 212*(3), 364–368.
Schuster, K. C., Ehmoser, H., Gapes, J. R., & Lendl, B. (2000). On-line FT-Raman spectroscopic monitoring of starch gelatinisation and enzyme catalysed starch hydrolysis. *Vibrational Spectroscopy, 22*(1), 181–190.
Sekkal, M., Dincq, V., Legrand, P., & Huvenne, J. P. (1995). Investigation of the glycosidic linkages in several oligosaccharides using FT-IR and FT Raman spectroscopies. *Journal of Molecular Structure, 349*, 349–352.
Seow, C. C., & Teo, C. H. (1996). Staling of Starch-based products: a comparative study by firmness and Pulsed NMR Measurements. *Starch-Stärke, 48*(3), 90–93.
Setser, C. S., & Racette, W. L. (1992). Macromolecule replacers in food products. *Critical Reviews in Food Science & Nutrition, 32*(3), 275–297.
Sigurgisladottir, S., Ingvarsdottir, H., Torrissen, O. J., Cardinal, M., & Hafsteinsson, H. (2000). Effects of freezing/thawing on the microstructure and the texture of smoked Atlantic salmon (Salmo salar). *Food Research International, 33*(10), 857–865.
Sworn, G., & Kasapis, S. (1998). Effect of conformation and molecular weight of cosolute on the mechanical properties of gellan gum gels. *Food Hydrocolloids, 12*(3), 283–290.
Thygesen, L. G., Løkke, M. M., Micklander, E., & Engelsen, S. B. (2003). Vibrational microspectroscopy of food. Raman vs. FT-IR. *Trends in Food Science & Technology, 14*(1), 50–57.

Tironi, V. A., Tomás, M. C., & Añón, M. C. (2010). Quality loss during the frozen storage of sea salmon (Pseudopercis semifasciata). Effect of rosemary (Rosmarinus officinalis L.) extract. *LWT-Food Science and Technology, 43*(2), 263–272.
Tu, A. T. (1982). *Raman spectroscopy in biology: Principles and applications* (p. 448). New York: John Wiley & Sons Ltd.
Van Soest, J. J. G., De Wit, D., Tournois, H., & Vliegenthart, J. F. G. (1994). Recrystallization of potato starch as studied by Fourier transform infrared spectroscopy. *Starch-Stärke, 46*(12), 453–457.
Yu, S., Ma, Y., & Sun, D. W. (2010). Effects of freezing rates on starch recrystallization and textural properties of cooked rice during storage. *LWT-Food Science and Technology, 43*(7), 1138–1143.